# Mechanistic Aspects Regarding the Ultraviolet Degradation of Polychlorinated Biphenyls in Different Media: Insights from Carbon and Chlorine Isotope Fractionation

Chenchen Huang, Yanhong Zeng,* Ya Cao, Chuhong Zhu, Zihe Ren, Yin-E Liu, Shutao Gao, Yankuan Tian, Xiaojun Luo, and Bixian Mai

Read Online

ACCESS | Metrics & More | Article Recommendations | Supporting Information

**ABSTRACT:** In this study, the carbon and chlorine isotope fractionation during ultraviolet-photolysis of polychlorinated biphenyls (PCBs, including PCB18, PCB77, PCB110, and PCB138) in n-hexane (Hex), methanol/water (MeOH/H$_2$O), and silica gel was first investigated to explore their mechanistic processes. We observed a significant variation in $\Lambda_{Cl-C}$ ($\varepsilon_{Cl}/\varepsilon_C$) for the same PCBs in different photochemical systems, implying that PCB degradation processes in various photoreaction systems could differ. Although all substrates showed normal apparent carbon/chlorine kinetic isotope effects (C−/Cl−AKIE >1), the putative inverse C-AKIE of nondechlorinated pathways was suggested by $^{13}$C depletion of the average carbon isotope composition of PCB138 and corresponding dechlorinated products in MeOH/H$_2$O, which might originate from the magnetic isotope effect. Significant negative correlations were found between C-AKIE and relative disappearance quantum yields ("Φ") of ortho-dechlorinated substrates (PCB18, PCB110, and PCB138) in Hex and MeOH/H$_2$O. However, the C-AKIE and "Φ" of PCB77 (meta/para-dechlorinated congener) obviously deviated from the above correlations. Furthermore, significantly different product-related carbon isotope enrichment factors of PCB77 in Hex were found. These results demonstrated the existence of dechlorination position-specific and masking effects in carbon isotope fractionations.

**KEYWORDS:** uv-photodegradation, polychlorinated biphenyls, compound-specific isotope analysis, carbon isotope fractionation, chlorine isotope fractionation, disappearance quantum yields, mechanistic process
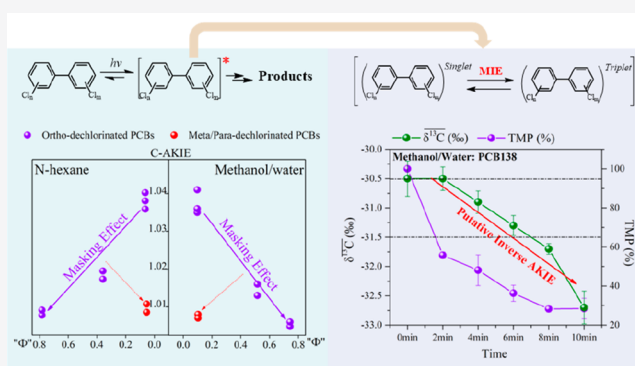
## INTRODUCTION

Light-induced transformation is an important natural attenuation of persistent organic pollutants (POPs).[1] A typical type of POP, polychlorinated biphenyls (PCBs), was previously used extensively as a hydraulic and dielectric fluid for transformers and capacitors.[2] Although the production and use of PCBs were forbidden 50 years ago, existing equipment that contains PCBs is allowed to be used until 2025.[3] In addition, the unintentionally produced PCB sources had been frequently found in air.[4,5] These imply that PCBs will remain in the environment for a long time, causing a threat to the ecology and human health.[5−8]

As regards remediation, several studies have demonstrated that PCBs could be degraded under ultraviolet (UV) and visible light irradiation.[9,10] The half-lives and degradation products associated with photodegradation of PCBs have been investigated systematically;[9,11] however, the detailed mechanistic processes, such as photoexcitation and bond breaking (or formation) processes from substrates to products, still remain unclear. Moreover, identification of photodegradation in the

field could be compromised by complicated PCB sources and other biological (or abiotic) processes occurring simultaneously with photochemical reactions.[12,13] Improved methods are therefore required to fill these research gaps.

Compound-specific isotope analysis (CSIA) can track variations in the stable isotope composition along with the transformation processes, which offers a new avenue to distinguishing different mechanistic pathways of degradation and assessing the fate of various contaminants in the environment.[12,14] Isotope fractionation is usually derived from bond changes, especially bond breaking in the rate-limiting step. This is called the kinetic isotope effect, which usually results in the enrichment of heavy isotopes in the

remaining substrates and the pathway-specific isotope enrichment factor.[15,16] However, there are possibly some additional effects, including (1) a masking effect to isotope fractionation caused by rate-limitations in the preceding process of isotope-sensitive bond cleavage, such as mass transfer[17] and (2) superimposed isotope effects of multistep chemical reactions.[18] These additional effects could lead to controversial interpretation of the experimental data with only single-element CSIA, as the isotope fractionation factor could be altered not only by the different mechanisms but also by these additional effects. It is worth noting that these additional effects usually synchronously change different elements and are almost counteracted with dual-element isotope plots $(\Lambda)$,[19−21] that is, graphs in which changes in isotope values of one element are plotted against those of a second. Hence, dual/multielement isotope analysis could provide a more reliable assessment about the underlying reaction mechanisms.

Dual/multidimensional CSIA (C−Cl, C−Br, and C−H−N) has been used widely to explore the (bio)degradation mechanisms of POPs, including the photolysis reactions of some organic compounds, such as brominated phenols, substituted chlorobenzenes, chloroanilines, and atrazine.[14,22−24] In this regard, Hartenbach et al. have reported completely opposite carbon/nitrogen isotope fractionation models between photo-oxidation and direct photolysis of atrazine.[24] Ratti et al. have demonstrated that both excited singlet and triplet states of 4-Cl-aniline could undergo heterolytic dechlorination and, furthermore, the linear correlations of apparent carbon versus nitrogen kinetic isotope effect (KIE) originating from these processes differ distinctly.[23] Furthermore, the magnetic isotope effect (MIE) has been proven to exist often in the photochemical reactions of organic contaminants, usually leading to anomalous inverse isotope fractionations.[14,24−27]

However, the focus of all the studies mentioned above was on the isotope fractionation of substrates. Little is known about the isotopic composition variation in products during photodegradation, except for the photolysis of polybrominated diphenyl ethers (PBDEs).[28,29] Given that most organic contaminants exist as intermediates in the field and the isotope fractionation of intermediates is controlled synchronously by bond breaking and formation, more key information could be obtained by researching isotope variation in products. Furthermore, light absorption leading to excitation of substrates, as the initialized step of direct photolysis, is considered a vital photochemical process that could affect isotope fractionation. Until now, no study has considered the influence of light absorption on isotope fractionation. N-hexane (Hex), methanol/water (MeOH/H_2O), and silica gel represented a nonpolar inert solvent, polar active solvent, and solid/air interface, respectively, which were three of the most popular photochemical systems to study the photodegradation of POPs in different media.[9,30−32] The UV-photodegradation products of PCBs in these three photodegradation systems had been comprehensively explored in our previous research[11] via selecting four dominant congeners with different chlorinated degrees in the environment (PCB18, PCB77, PCB110, and PCB138) as model compounds. However, the isotopic fractionation in the photodegradation of PCBs and its mechanism are still unclear.

Therefore, in the current study, we further explored the mechanistic aspects of the UV-degradation of PCBs (including PCB18, PCB77, PCB110, and PCB138) in Hex, MeOH/H_2O,

and silica gel systems using compound-specific dual carbon/chlorine isotope analysis (C−/Cl−CSIA). The observed carbon/chlorine isotope fractionation of both substrates and dechlorination products was investigated. In addition, we evaluated the disappearance quantum yield of substrates, as it is a meaningful parameter connecting light excitation with bond breaking. Our work was devoted to providing more mechanistic interpretation to photodegradation pathways of PCBs in various media and evaluating the potential of CSIA for photodegradation of PCBs in the field.

## ■ MATERIALS AND METHODS

**Chemicals.** We obtained photodegradation substrates, including PCB18, PCB77, PCB110, and PCB138, from AccuStandard Inc. (USA). Their structures are given in Figure S1 in the Supporting Information (SI). Silica gel (80−100 mesh) was purchased from Qingdao Haiyang Chemical Co., Ltd. (China). HPLC-grade n-hexane (Hex) and methanol were provided by CNW Technologies Co., Ltd. (Germany).

**Photodegradation Procedure.** We conducted the UV-photolysis experiments using a BL-GHX-V photochemical reactor (Shanghai Bilon Instrument Co., Ltd., China), with a high-pressure mercury lamp (100 W). A detailed description of the photodegradation processes had been published in our another paper[11] and is available in the Supporting Information.

**Sample Pretreatment and CSIA.** The methods of sample pretreatment and compound-specific carbon/chlorine isotope analysis (C−/Cl−CSIA) had been published in our previous literature.[11,12,33] They were also described in the Supporting Information in detail. Briefly, after extraction, nine-tenths of the extract was redissolved in 50 $\mu$L isooctane for C-CSIA, and one twenty-fifth of the extract was reconstituted in 300 $\mu$L isooctane for Cl-CSIA.

The C-CSIA of PCB congeners was performed using a trace gas chromatography (GC) Ultra-IsoLink Delta V Advantage isotope ratio mass spectrometer (IRMS) (Thermo-Fisher Scientific) coupling a DB-5 MS chromatographic column (60 m, 250 $\mu$m i.d., and 0.25 $\mu$m film thickness). For Cl-CSIA, a GC-quadrupole mass spectrometry (qMS) system (Agilent 7890A-5975C) coupling a DB-5MS capillary column (30 m, 250 $\mu$m i.d., and 0.25 $\mu$m film thickness) was used. All of the chlorine isotope ratios were calculated using the molecular ion method.[33] Each sample was injected 10 times, and the data were only considered for their standard deviations of chlorine isotope ratios in 10 injections less than 0.00068.[33] Considering that $^{13}$C-correction for chlorine isotope compositions ($^{37}$Cl/$^{35}$Cl) has no alteration in $^{37}$Cl/$^{35}$Cl variation patterns and isotope enrichment factors,[33] in the current study, all the $^{37}$Cl/$^{35}$Cl values were evaluated without $^{13}$C-correction.

**Isotope Data Analysis.** The stable carbon isotope compositions ($\delta^{13}$C) are calculated as follows (eq 1):

$$\delta^{13}C\ (\permil) = ((R_{sample}/R_{standard}) - 1) \times 1000 \qquad (1)$$

where $R_{sample}$ and $R_{standard}$ are the $^{13}$C/$^{12}$C values of the samples and the international standard Vienna Pee Dee Belemnite (V-PDB), respectively. The stable chlorine isotope compositions are expressed directly as the "raw" $^{37}$Cl/$^{35}$Cl ratios, without correcting to the standard mean ocean chloride (SMOC) scale because of the lack of international standards.

Bulk carbon and chlorine isotopic enrichment factors ($\varepsilon_C$ and $\varepsilon_{Cl}$) are determined using the following Rayleigh equation (eq 2):
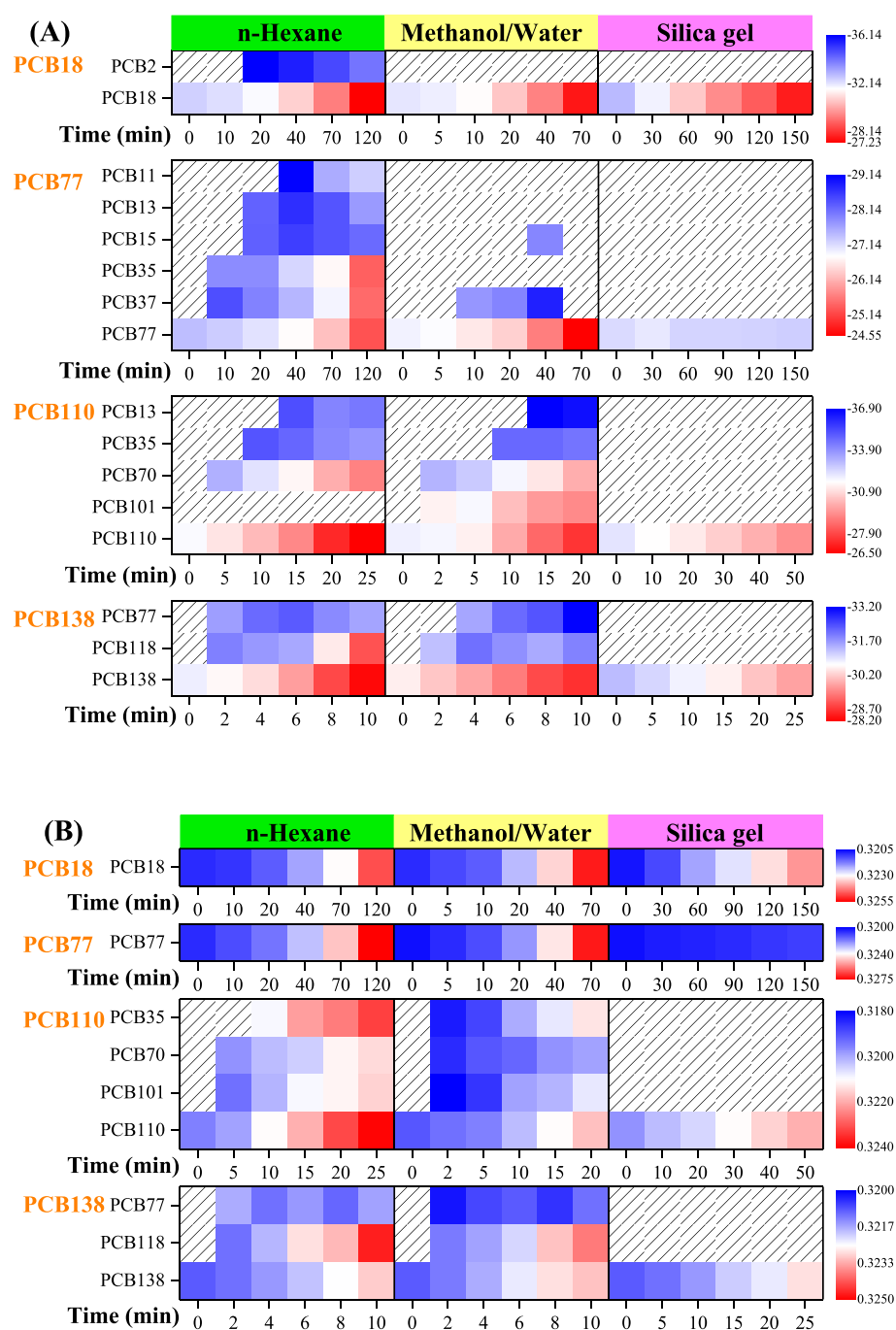
**Figure 1.** $\delta^{13}$C (Panel A) and $^{37}$Cl/$^{35}$Cl (Panel B) variation in photochemical substrates, rearrangement, and dechlorination products in Hex, MeOH/H$_2$O, and silica gel systems.

$$Ln\left(\frac{R_t}{R_0}\right) = \frac{\varepsilon}{1000} \times Lnf \qquad (2)$$

where $R_0$ and $R_t$ are the isotope ratios ($^{13}$C/$^{12}$C for $\varepsilon_C$ and $^{37}$Cl/$^{35}$Cl for $\varepsilon_{Cl}$) at the initial time 0 min and sampling time t min, respectively, and $f$ is the ratio of the concentration of the substrate at time t min relative to its concentration at 0 min.
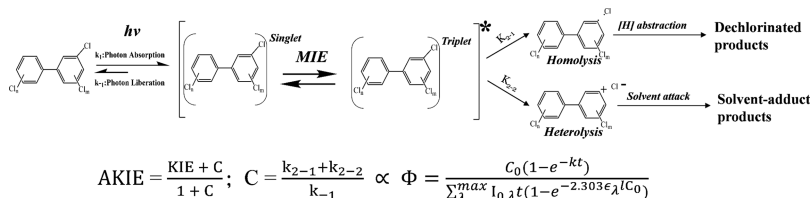
For further discriminating the reaction mechanism, the $\varepsilon_C$ and $\varepsilon_{Cl}$ are converted to the apparent carbon and chlorine KIE (C-AKIE and Cl-AKIE), respectively. The conversion equation was as follows (eq 3):

$$AKIE = \frac{1}{1 + z \times (n/x) \times \varepsilon/1000} \qquad (3)$$

where $n$, $x$, and $z$ are the number of carbon or chlorine atoms in the molecule, at reactive positions, and at equivalent reactive positions, respectively. Given the stepwise dechlorination of PCBs under UV-irradiation, $x$ is considered equal to $z$ for the studied PCB congeners.

To provide an evaluation parameter that is more sensitive to differentiating reaction mechanisms, the slope of dual-element isotope plots ($\Lambda$) was calculated using the following equation (eq 4):

**Scheme 1. Possible Mechanistic Scenarios for UV-Degradation of PCBs**



$$AKIE = \frac{KIE + C}{1 + C}; \quad C = \frac{k_{2-1} + k_{2-2}}{k_{-1}} \propto \Phi = \frac{C_0(1 - e^{-kt})}{\sum_{\lambda}^{max} I_{0,\lambda} t(1 - e^{-2.303\epsilon_\lambda l C_0})}$$

$$\Lambda_{Cl-C} = \frac{\delta^{13}Cl - \delta^{13}Cl_0}{\delta^{13}C - \delta^{13}C_0} \approx \frac{\varepsilon_{Cl}}{\varepsilon_C} = \frac{Ln\left(\frac{R_t}{R_0}\right)_{Cl}}{Ln\left(\frac{R_t}{R_0}\right)_C} \quad (4)$$

where $Ln(R_t/R_0)_{Cl}$ and $Ln(R_t/R_0)_C$ are the $Ln(R_t/R_0)$ values of carbon and chlorine elements, respectively.

**Quality Assurance/Quality Control.** Complete quality assurance/quality control procedures were conducted along with the experimental process. To ensure the accuracy of the experimental results, all the photodegradation of PCBs was conducted in a set of three groups of parallel experiments, with one group of control experiments with dark treatment. In the instrumental analysis process, a PCB standard mixture (containing PCB18, PCB77, PCB 110, and PCB138) was detected daily to ensure the stability of the instrument, and no significant variations were observed for carbon and chlorine isotope ratios of the PCB standard mixture. Prior to C-CSIA, a coinjected standard (PCB30) was added to the samples. The $\delta^{13}C$ values of the PCB30 measured online (−29.08 to −28.75‰) were close to the true values (−28.80‰, determined off-line using a Flash 2000 EA-Delta V Plus IRMS [Thermo-Fisher Scientific, USA]).

**Statistical Analysis.** The statistical analysis was performed using SPSS 22.0 and Origin 9.0. The statistical differences between the evaluation parameters for isotope fractionation were evaluated using one-way analysis of variance (ANOVA), with a posthoc Tukey's honest significant difference test. Correlation analysis (Person) was performed to assess the relationships between the AKIE and the observed first-order rate constants ($k_{obs}$), or AKIE and the relative disappearance quantum yields ("Φ"). The significance level was set at $p < 0.05$ in the current study.

■ **RESULTS AND DISCUSSION**

**Compound-Specific Carbon and Chlorine Isotope Signature Variations.** No carbon and chlorine isotope fractionation of PCB substrates was detected throughout the dark control groups. Except $\delta^{13}C$ of PCB77 in silica gel, both the carbon and chlorine isotope compositions of PCB18, PCB77, PCB110, and PCB138 in Hex, MeOH/H$_2$O, and silica gel systems had heavy isotope ($^{13}C$ and $^{37}Cl$) enrichment along with the UV-irradiation times (Figure 1, Table S1 and S2). These heavy isotope enrichment trends were in accordance with the concentration decrease in the substrates[11] (Figure S2 and Table S3), suggesting that PCB photodegradation results in normal isotope fractionation of PCBs.

The photodegradation products were determined using mass spectra analysis in our previous study.[11] The substrates in the Hex, MeOH/H$_2$O, and silica gel systems were mainly degraded to lower chlorinated PCBs, lower chlorinated PCBs/methoxylated PCBs (CH$_3$O-PCBs)/hydroxylated PCBs (OH-PCBs), and OH-PCBs, respectively.[11] In addition,

there were also some minor products generated from the photodegradation of PCBs, including methylated PCBs, polychlorinated dibenzofurans, and polychlorinated biphenyl ethers.[11] Our results suggested that the degradation processes of PCBs in the studied three media were complicated.[11] The potential reaction pathways to dechlorination and sigmatropic rearrangement products in Hex and MeOH/H$_2$O systems[11] are given in Figure S3. The ortho-chlorine atoms were most easily dechlorinated followed by meta- and para-chlorine atoms.

The $\delta^{13}C$ values of 12 dechlorinated products in Hex (one, five, four, and two for PCB18, PCB77, PCB110, and PCB138, respectively) and 8 dechlorinated products in MeOH/H$_2$O (two, four, and two for PCB77, PCB110, and PCB138, respectively) were detected (Figure 1A and Table S1), which regularly showed $^{13}C$ depletion relative to their corresponding substrates. The $\delta^{13}C$ values of most products usually had synchronous $^{13}C$ enrichment trends with their substrates throughout UV-irradiation. However, some products in MeOH/H$_2$O, such as PCB37 from PCB77 and PCB118/77 from PCB138, showed significant $^{13}C$ depletion trends or no significant carbon isotope fractionation, which were different from those in Hex (Figure S2A). In principle, an organic compound could undergo homolysis and heterolysis to break bonds and generate different products after photoexcitation. Research has indicated that chlorinated aromatic compounds usually produce dechlorinated products through homolysis of the C−Cl bond followed by free radical hydrogen abstraction from the hydrogen donor.[34] Alternatively, such compounds are translated to hydroxylated products induced by heterolytic aryl-chlorine bond cleavage followed by solvent attack on the aryl cation.[34] Zakon et al. found that there were different carbon isotope fractionations between homolysis and heterolysis of the C−Br bond upon UV-degradation of brominated phenols.[14] PCBs mainly experience dechlorination in Hex, whereas PCBs occur dechlorination, methoxylation, and hydroxylation simultaneously in MeOH/H$_2$O[11]. Accordingly, we assumed that PCBs would be photodegraded to dechlorination and solvent-adduct products through homolysis and heterolysis of aryl-chlorine bonding, respectively (Scheme 1), leading to different isotope fractionation. More complicated isotopic kinetic processes could occur in MeOH/H$_2$O than in Hex.

In addition, the $^{37}Cl/^{35}Cl$ values of most main dechlorinated products were determined for PCB110 and PCB138 in the Hex and MeOH/H$_2$O systems (Figure 1B and Table S2). Most of the photodegradation products (PCB101/70/35 from PCB110 and PCB118 from PCB138) showed $^{37}Cl$ enrichment as the reaction continued. However, the PCB77 in PCB138/MeOH/H$_2$O and PCB138/Hex systems had no chlorine isotope fractionation (Figure S2B). Photodegradation of PCB138 usually had a single main dechlorination pathway in Hex and MeOH/H$_2$O, as PCB138 → PCB118 → PCB77, and
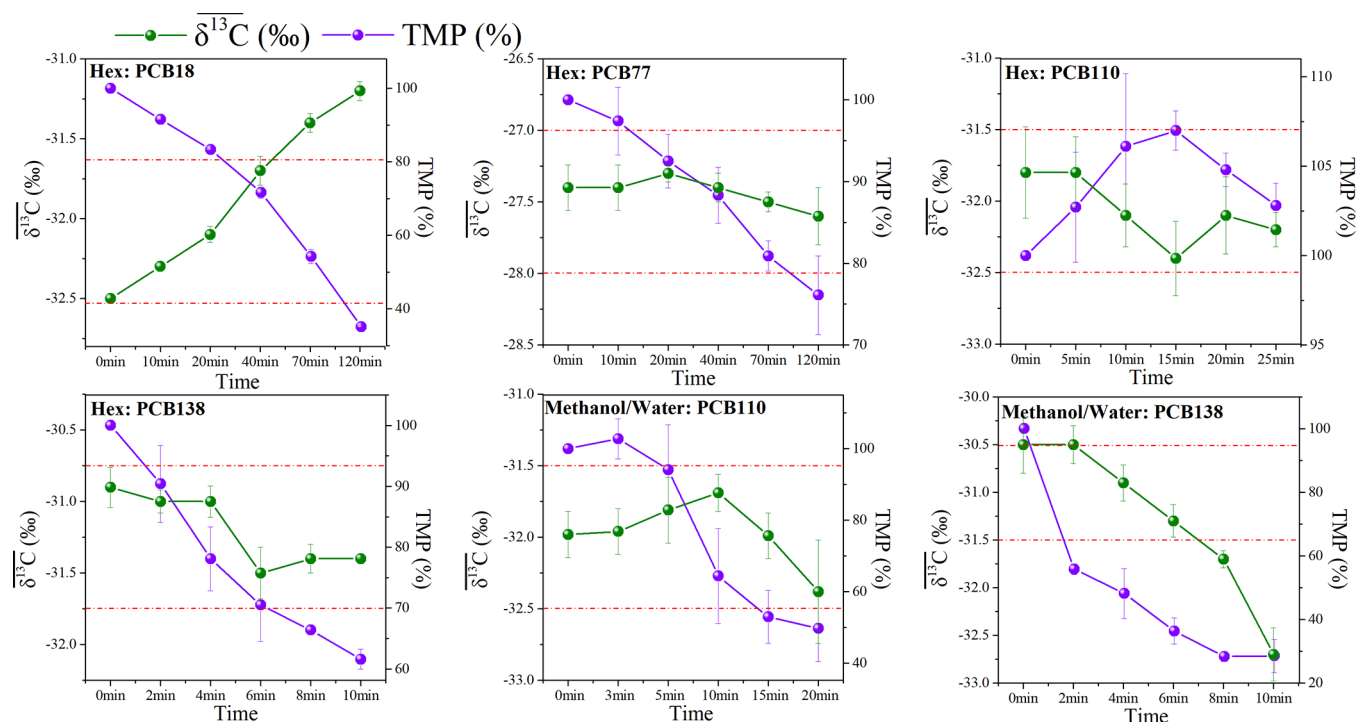
**Figure 2.** Variation in $\delta^{13}\overline{C}$ and TMP (%) along with the UV-irradiation times. $\delta^{13}\overline{C}$ represents the average $\delta^{13}C$ values of substrates and their corresponding dechlorination products, and TMP represents the total molar percent of substrates and their corresponding dechlorination products relative to the initial substrate.

the chlorine atoms of PCB138 and PCB118 are not chemically equivalent (Figure S3). Assuming that secondary isotope effects are absent and only one of the six positions of PCB138 or one of the five positions of PCB118 undergoes dechlorination, the chlorine isotope composition at non-reactive positions remains constant because of no occurrence of isotope enrichment or depletion.[35] Therefore, the chlorine isotope composition of dominating intermediates (e.g. PCB77) mainly changed by the degradation of themselves.[35] From our previous study, we found that PCB77 was mainly formed while its degradation was very slow.[11] Obviously, the insignificant chlorine isotope fractionation of dechlorination product PCB77 could be ascribed to minor degradation of PCB77 itself.[11]

*Correlation of $\delta^{13}C$ Values and Dechlorination Degree.* As shown in Figure S4, UV-induced dechlorination resulted in significantly positive correlations between the degree of chlorination and the $\delta^{13}C$ values of PCBs, which was reversed with the intrinsic isotope trend of $^{13}C$ depletion along with increasing chlorine content in Aroclor mixtures.[36] Therefore, the slope of the relationship between carbon isotope signatures and the chlorination degree could be used to trace the degradation of PCBs in the field. This finding is in accordance with the carbon isotope variations of PBDEs under light-induced degradation.[28,29]

*Potential MIE Revealed by Isotope Mass Balance.* To further explore the difference in isotope fractionation among different photodegradation processes, we calculated the average $\delta^{13}C$ values ($\delta^{13}\overline{C}$) of substrates and their corresponding dechlorination products for each sampling point of PCB18/77/110/138 in Hex and PCB110/138 in MeOH/H$_2$O. These could reflect the isotope variation in non-dechlorination products based on isotope mass balance (Figure 2). In addition, the total molar percent of the substrate and

corresponding dechlorination products relative to the initial substrate (TMP, %) were also calculated for each sampling point of PCB18/77/110/138 in Hex and PCB110/138 in MeOH/H$_2$O. Details of the calculation methods of $\delta^{13}\overline{C}$ and TMP are presented in the Supporting Information. The basic data set and the calculation processes are also given in the Supporting Information (Microsoft Excel 2019). As shown in Figure 2, the system of PCB110/Hex showed molar number balance and carbon isotope mass balance when only the PCB110 and dechlorination products were considered. However, the TMP for PCB18/77/138 in Hex and for PCB110/138 in MeOH/H$_2$O gradually decreased along with the UV-irradiation times (Figure 2). These decreases were caused by the generation of biphenyls and nondechlorination products, including n-hexylated PCBs ($n-C_6H_{13}-PCBs$), $CH_3O-PCBs$, and $OH-PCBs$.[11] On the other hand, as the reaction continued, the trends of $\delta^{13}\overline{C}$ varied depending on the substrates and UV-irradiation systems. The $\delta^{13}\overline{C}$ for PCB18 in Hex significantly increased, which is a normal trend because of the generation of many biphenyls preferentially carrying $^{12}C$ off.[11] However, the $\delta^{13}\overline{C}$ for PCB77/138 in Hex and PCB110 in MeOH/H$_2$O remained nearly constant, with the range-ability less than 1‰. In particular, the $\delta^{13}\overline{C}$ for PCB138 in MeOH/H$_2$O had a significant decrease trend, with the $\delta^{13}\overline{C}$ change being greater than 2‰ (Figure 2). This phenomenon implied that nondechlorination pathways, such as n-hexylation, hydroxylation, and methoxylation, resulted mostly in no or inverse carbon isotope fractionation, which obviously differ from the dechlorination process. However, these no or inverse isotope effects proved by the variations of the $\delta^{13}\overline{C}$ need further verification, because the $\delta^{13}\overline{C}$ was derived from complicated calculation rather than measurement directly. There might be an error because of the uncertainty of concentrations and simulative $\delta^{13}C$ values of some PCBs.

**Table 1. Carbon and Chlorine Isotope Enrichment Factors ($\varepsilon_C$ and $\varepsilon_C$, respectively), Apparent Carbon and Chlorine Kinetic Isotope Effects (C-AKIE and Cl-AKIE, respectively), Dual Isotope Slopes ($\Lambda_{Cl\text{-}C}$), Observed First-Order Rate Constants ($k_{obs}$), and Relative Disappearance Quantum Yields ("$\Phi$") Obtained for the UV-Photolysis of PCB18, PCB77, PCB110, and PCB138 in N-Hexane (Hex), Methanol/Water (MeOH/H$_2$O), and Silica Gel Systems**

| | | $\varepsilon_C$ | $\varepsilon_{Cl}$ | C-AKIE | Cl-AKIE | $\Lambda_{Cl\text{-}C}$ | $k_{obs}$ (min$^{-1}$) | "$\Phi$" |
|---|---|---|---|---|---|---|---|---|
| PCB18 | Hex | −2.83 ± 0.15 | −6.13 ± 0.31 | 1.0352 ± 0.0020 | 1.0187 ± 0.0010 | 2.16 ± 0.05 | 0.0168 | 0.064 |
| | MeOH/H$_2$O | −3.00 ± 0.26 | −8.47 ± 0.31 | 1.0374 ± 0.0034 | 1.0261 ± 0.0010 | 2.83 ± 0.14 | 0.0227 | 0.098 |
| | silica gel | −3.03 ± 0.06 | −5.93 ± 0.06 | 1.0378 ± 0.0007 | 1.0181 ± 0.0002 | 1.95 ± 0.06 | 0.0114 | |
| PCB77 | Hex | −0.73 ± 0.06 | −7.07 ± 0.12 | 1.0089 ± 0.0007 | 1.0291 ± 0.0005 | 9.75 ± 0.39 | 0.0265 | 0.055 |
| | MeOH/H$_2$O | −0.67 ± 0.06 | −5.87 ± 0.15 | 1.0081 ± 0.0007 | 1.0240 ± 0.0006 | 8.61 ± 0.34 | 0.0533 | 0.103 |
| | silica gel | ND$^a$ | −4.17 ± 0.15 | | 1.0169 ± 0.0006 | | 0.0036 | |
| PCB110 | Hex | −1.43 ± 0.12 | −3.67 ± 0.12 | 1.0175 ± 0.0014 | 1.0187 ± 0.0006 | 2.55 ± 0.32 | 0.1682 | 0.358 |
| | MeOH/H$_2$O | −1.23 ± 0.12 | −2.17 ± 0.06 | 1.0150 ± 0.0014 | 1.0110 ± 0.0003 | 1.77 ± 0.15 | 0.2114 | 0.516 |
| | silica gel | −1.47 ± 0.06 | −3.53 ± 0.15 | 1.0179 ± 0.0007 | 1.0180 ± 0.0008 | 2.37 ± 0.10 | 0.0398 | |
| PCB138 | Hex | −0.67 ± 0.06 | −1.57 ± 0.06 | 1.0081 ± 0.0007 | 1.0095 ± 0.0004 | 2.42 ± 0.25 | 0.5178 | 0.782 |
| | MeOH/H$_2$O | −0.47 ± 0.06 | −1.63 ± 0.12 | 1.0056 ± 0.0007 | 1.0099 ± 0.0007 | 3.72 ± 0.09 | 0.4590 | 0.743 |
| | silica gel | −0.70 ± 0.00 | −2.50 ± 0.10 | 1.0085 ± 0.0000 | 1.0152 ± 0.0006 | 3.56 ± 0.14 | 0.0995 | |

$^a$ND, not detected.

Therefore, further studies need to be performed, such as using liquid chromatography interfaced with isotope ratio mass spectrometry to measure the $\delta^{13}$C values of OH−PCBs[37] and using site-specific natural isotope fractionation coupled nuclear magnetic resonance to detect the $\delta^{13}$C values at the reactive site of CH$_3$O−PCBs and n−C$_6$H$_{13}$-PCBs,[38] which could provide direct evidence for inverse isotope effects existing in nondechlorination pathways. Anyhow, this developed a new clue for studying isotope fractionation of different pathways in the complex degradation process and highlighted the importance of the product isotope analysis.

Zakon et al. have reported that 2-bromophenol and 3-bromophenol mainly experienced hydroxylation in the UV-irradiation/water system, with no carbon isotope fractionation detected in this process.[14] Moreover, Wang et al. have demonstrated inverse carbon isotope fractionation during light-induced hydroxylation of tribromobisphenol A.[25] Previous research studies' general thought is that inverse isotope effects during photoreactions were caused by the MIE.[14,24−27] The MIE is the mass-independent isotope effect, originating from preferential selectivity for singlet−triplet states conversion of different magnetic isotopes, which often exist in photochemical reaction processes.[24,25] Therefore, this putative inverse isotope fractionation for nondechlorination pathways of PCB138 in MeOH/H$_2$O probably implied the occurrence of the MIE in intersystem-crossing of singlet−triplet states. The above analysis has suggested that PCBs could simultaneously undergo homolysis and heterolysis of the C−Cl bond to generate dechlorinated and solvent-adduct products, respectively, which could initiate from different light-excited states (singlet or triplet states) to result in the MIE[14] (Scheme 1). In addition, PCBs were possibly excited to singlet and triplet states concurrently and, then, returned to the ground state by various photophysical processes, which also might cause inverse isotope fractionation.[24,39] The mechanism behind inverse isotope fractionation during the photodegradation process needs to be further explored.

**Isotope Enrichment Factor and AKIEs.** The $\varepsilon_C$ and $\varepsilon_{Cl}$ of PCB18, PCB77, PCB110, and PCB138 in the three photochemical systems were calculated according to eq 2 and are presented in Figure S5 and Table 1. Although the chlorine isotope ratios of PCBs were determined without correcting to the SMOC scale, the raw $\varepsilon_{Cl}$ could still provide

useful information on mechanism analysis for the same PCBs in different photochemical systems because GC-qMS commonly has the constant bias or drift on $^{37}$Cl/$^{35}$Cl ratios of the same compounds. However, it was meaningless to compare the raw $\varepsilon_{Cl}$ of different compounds because of the calibration slopes of raw $^{37}$Cl/$^{35}$Cl ratios against the SMOC scale varying among different compounds.[40] The $\varepsilon_C$ and $\varepsilon_{Cl}$ of the studied PCBs in the three photochemical systems ranged from −0.47 ± 0.06 to −3.03 ± 0.06‰ and from −1.57 ± 0.06 to −8.47 ± 0.31‰, respectively (Table 1). Generally, the influence of photochemical systems for a given PCB congener is much larger on $\varepsilon_{Cl}$ than on $\varepsilon_C$ (Figure S5). One standard deviation (+1$\sigma$) was once used to determine whether there was a difference among various isotope enrichment parameters in previous literature.[24] In the current study, the $\varepsilon_C$ of PCB18/77 in different photochemical systems was identical within +1$\sigma$. The differences for $\varepsilon_C$ of PCB110/138 and for $\varepsilon_{Cl}$ of PCB18/77/110/138, in contrast, were larger than the corresponding +1$\sigma$ (Table 1). In addition, the statistical differences of $\varepsilon_C$ and $\varepsilon_{Cl}$ for the same PCB substrate in the three photochemical systems were evaluated by one-way ANOVA. There were no statistical differences for $\varepsilon_C$ of PCB18/77/110 among different photodegradation systems (ANOVA, $p > 0.05$), suggesting that the bond breaking of C−Cl was the rate-limiting step. However, significant differences were observed for $\varepsilon_C$ of PCB138 and $\varepsilon_{Cl}$ of PCB18/77/110/138 (ANOVA, $p < 0.05$), and the orders of size for $\varepsilon_C$ and $\varepsilon_{Cl}$ varied with the PCB substrates (Figure S5). Variations in $\varepsilon$ were also found for bromophenol photodegradation in ethanol and water, which might be caused by different bond breaking processes of C−Br.[14] Ratti et al. have demonstrated that the dechlorination photolysis of 4-chlorianiline from excited triplet states could cause larger carbon and nitrogen isotope fractionation compared with those from excited singlet states.[23] Based on the above analysis, the observed isotope enrichment factors were probably controlled by the bond breaking ways (homolysis or heterolysis) and excited states for bond cleavage (Scheme 1), which could result in different kinetic and magnetic isotope effects. This finding indicates that the photodegradation processes of PCBs are extremely complicated, and differences could exist for the same substrates in different photodegradation systems. In addition, the $\Lambda_{Cl−C}$ values were gained via carbon and chlorine isotope plots
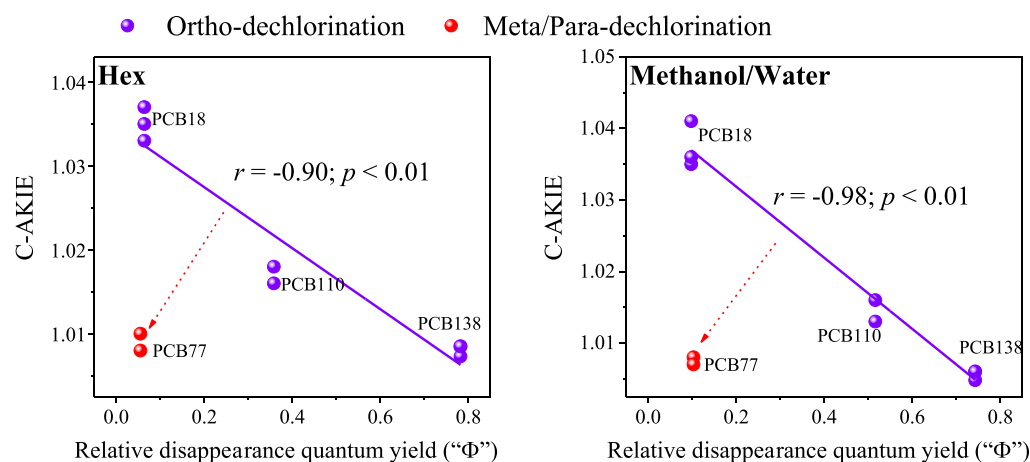
**Figure 3.** Correlation between apparent carbon kinetic isotope effects (C-AKIE) and the relative disappearance quantum yield ("Φ") of PCBs (correlation analysis based on the data of PCB18, PCB110, and PCB138).

(Figure S6). For a specific substrate in the three photodegradation systems, the differences of $\Lambda_{Cl-C}$ between each other were significant (AONVA, $p < 0.01$) and all larger than the $+1\sigma$, which further proved that the degradation mechanisms were different in the three studied systems (Table 1).

Although the isotope enrichment factor is a useful evaluation parameter for degradation processes, it does not reflect the isotope effects in reacting bonds. To further elucidate the degradation mechanisms, the $\varepsilon_C$ and $\varepsilon_{Cl}$ were transformed into C-AKIE and Cl-AKIE, respectively. The magnitudes of the observed C-AKIE ranged from $1.0056 \pm 0.0007$ to $1.0378 \pm 0.0007$ (Table 1), which were within the C-AKIE range for the C−Cl bond cleavage upon biotic or abiotic degradation reported in the literature (1.001−1.072).[41] The largest C-AKIE values were achieved on PCB18 (1.0352−1.0378), similar to C-KIE for approximately 50% C−Cl bond breaking when considering the maximum KIE (Streitwieser Semiclassical Limits) of 1.057 with complete cleavage of the C−Cl bond in an infinitely late transition state.[42] However, the C-AKIE values of PCB77, PCB110, and PCB138 were much less than those of PCB18 (Table 1).

Regarding Cl-AKIE, a range of $1.0095 \pm 0.0004$ to $1.0291 \pm 0.0005$ was calculated, of which most were larger than the published Cl-AKIE for C−Cl bond cleavage in chlorinated aliphatic compounds (1.004−1.016)[41] and the Streitwieser Semiclassical Limits for Cl-KIE in C−Cl bonds (1.013).[42] These anomalies were possibly caused by the following two reasons: (1) the $\varepsilon_{Cl}$ was calculated using the raw $^{37}Cl/^{35}Cl$ ratios, which were not corrected to the SMOC scale and (2) the Streitwieser Semiclassical Limits were determined without considering the influence of molecular masses, moments of inertia, and tunneling to isotope effects.[42] More research on chlorine isotope fractionation upon photolysis of PCBs needs to be applied with advanced equipment, such as GC-multiple collector inductively coupled plasma mass spectrometry.[43]

*Masking Effect Caused by Limited Photon Absorption.* The significantly negative correlation between C-AKIE and first-order rate constants ($k_{obs}$) for ortho-dechlorinated substrates (PCB18, PCB110, and PCB138) in the three photochemical systems implied that isotope fractionation might be influenced by the masking effect[22] (Figure S7). As regards photochemical reactions, the ground state substrates first are excited to excited states after absorbing light of a

particular wavelength. Subsequently, the excited state substrates not only could be transformed to aryl cations or radicals through C−Cl bond breaking but also could return to the ground state by emitting phosphorescence or fluorescence (Scheme 1). Therefore, the magnitudes of the AKIE were influenced by the ratio of the bond breaking rate constants ($k_{obs} \approx k_{2-1} + k_{2-2}$) to the photon absorption rate constant ($k_1$) (Scheme 1). To express this masking effect clearly, a commitment factor, C, was introduced to establish a connection between AKIE and KIE.[42] As shown in Scheme 1, when $k_1 >> k_{2-1} + k_{2-2}$, C is infinitely close to 0 and there is no masking effect (AKIE = KIE); however, when $k_1 \approx k_{2-1} + k_{2-2}$, C approaches infinity and isotope fractionation is masked completely (AKIE = 1). Here, C is equivalent to the disappearance quantum yield (Φ). We determined the relative intensity of emission light from the 100 W high-pressure mercury lamp ($I_0$) and the molar absorption coefficient on different wavelengths ($\varepsilon_\lambda$) for the studied PCB substrates in Hex and MeOH/H$_2$O systems to calculate the relative disappearance quantum yields ("Φ")[44] (Figure S8 and Table 1). As expected, C-AKIE and "Φ" of the ortho-dechlorinated substrates (PCB18, PCB110, and PCB138) in Hex and MeOH/H$_2$O systems had a significantly negative correlativity, demonstrating the presence of a masking effect that reduced carbon isotope fractionations upon UV-photolysis of PCBs (Figure 3). Although similar negative correlativity also existed between Cl-AKIE and $k_{obs}$ (or "Φ") of the ortho-dechlorinated substrates (PCB18, PCB110, and PCB138), they were not further discussed because of the limitations from the raw $^{37}Cl/^{35}Cl$ ratios (Figure S9).

*Dechlorination Position-Specific Isotope Fractionation.* In particular, C-AKIE and "Φ" of PCB77, the meta/para-dechlorinated substrate, were unmatched to the trends of the AKIE & "Φ" fitting with ortho-dechlorinated substrates. This finding suggested that carbon isotope fractionation is dechlorination position-specific for PCBs, which might result from the difference of C−Cl bond dissociation energy in different substitution positions (Figure 3). The same mechanism was also concealed in photodegradation of PBDEs.[28] PCB77 could simultaneously undergo meta-dechlorination (PCB77 → PCB37 → PCB15) and para-dechlorination (PCB77 → PCB35 → PCB13/11) upon UV-irradiation. Here, the photodegradation of PCB77 in Hex was selected to further explore dechlorination position-specific of

the carbon isotope effect because of the following advantages: (1) meta-/para-dechlorination is the main degradation pathway, with the other pathways having almost no influence on carbon isotopic mass balance and (2) the $\delta^{13}$C values of all main products (PCB37, PCB35, PCB15, PCB13, and PCB11) were determined. As shown in Figure S10, the isotope fractionations from PCB77 to meta- and para-dechlorinated products were markedly different. The product-related isotope enrichment factors, $\varepsilon_{C, PCB77 \to meta}$ and $\varepsilon_{C, PCB77 \to para}$, were estimated as $-1.13 \pm 0.08\%o$ and $-0.57 \pm 0.29\%o$, respectively, using methods described in previous literature.[45] Our results provided powerful evidence of the dechlorination position-specific in the isotope effect.

**Environmental Significance.** In the current study, the carbon and chlorine isotope effects during UV-photodegradation of PCBs in Hex, MeOH/H$_2$O, and silica gel were explored for the first time. Considering that UV-induced degradation of PCBs could provide a potential remediation method for PCB contamination, the $\varepsilon_C$ and $\varepsilon_{Cl}$ values determined in our study could be used to quantify the degree of degradation without influence from physical processes. However, for the field environment, the far ultraviolet (UV-C; 200-280 nm) in solar light, degrading PCBs directly, can hardly reach the surface of the earth. PCBs possibly mainly undergo indirect photodegradation in the field. Therefore, further research regarding the isotope effects during the indirect photodegradation of PCBs is urgent to be carried out for better understanding the fate of PCBs in the field.

Meanwhile, this work is the first to mention that the disappearance quantum yields could cause masking of the isotope effects during light-induced degradation of POPs. Given the differences between field and laboratory environments, there might be different degrees of masking effect, resulting in the alteration of isotope enrichment factors. Therefore, we should be careful about using isotope enrichment factors obtained in the laboratory to evaluate the degradation degree of PCBs in the field contamination remediation project. In addition, the finding of masking effect suggested that it is more reliable to evaluate photodegradation mechanisms of PCBs using dual-element isotope enrichment factors than one-element isotope enrichment factors. Moreover, unlike previous studies that focused mainly on the isotope fractionation of substrates, the present study determined the isotope composition of both substrates and products, which could generate more mechanistic information. For example, although all the studied substrates experienced heavy isotope enrichment, showing normal KIEs upon UV-irradiation, the average isotope composition variations in substrates and products could provide insight into the inverse KIE, suggesting the occurrence of the MIE. This finding demonstrates the significant effect of product isotope analysis and develops a new clue for mechanism study using CSIA.

## ASSOCIATED CONTENT

### Ⓢ Supporting Information

The Supporting Information is available free of charge at https://pubs.acs.org/doi/10.1021/acs.est.1c00726.

Photodegradation procedure, sample pretreatment, the calculation methods of $\overline{\delta^{13}C}$ values, molecular structural formulas of the four studied PCBs, potential reaction pathways, Correlation between $\delta^{13}$C values and degree of chlorination, Rayleigh plots, dual-element isotope

plots, molar absorption coefficient of studied PCBs, correlation between C-AKIE and rate constants of PCBs, product-related isotope fractionation, $\delta^{13}$C and $^{37}$Cl/$^{35}$Cl values of photochemical substrates and dechlorinated products, and relative concentrations data of substrates (PDF)

The detailed calculation process of TMP(%) and ($\overline{\delta^{13}C}$) (XLSX)

## AUTHOR INFORMATION

### Corresponding Author

**Yanhong Zeng** − *Guangdong-Hong Kong-Macao Joint Laboratory for Environmental Pollution and Control and State Key Laboratory of Organic Geochemistry and Guangdong Key Laboratory of Environmental Protection and Resources Utilization, Guangzhou Institute of Geochemistry, Chinese Academy of Sciences, Guangzhou 510640, China; CAS Center for Excellence in Deep Earth Science, Guangzhou 510640, China;* ⓞ orcid.org/0000-0002-8850-2456; Phone: +86-020-85291509; Email: zengyh@gig.ac.cn; Fax: 86-020-85290706

### Authors

**Chenchen Huang** − *State Key Laboratory of Organic Geochemistry and Guangdong Key Laboratory of Environmental Protection and Resources Utilization, Guangzhou Institute of Geochemistry, Chinese Academy of Sciences, Guangzhou 510640, China; CAS Center for Excellence in Deep Earth Science, Guangzhou 510640, China; University of Chinese Academy of Sciences, Beijing 100049, China*

**Ya Cao** − *State Key Laboratory of Organic Geochemistry and Guangdong Key Laboratory of Environmental Protection and Resources Utilization, Guangzhou Institute of Geochemistry, Chinese Academy of Sciences, Guangzhou 510640, China; CAS Center for Excellence in Deep Earth Science, Guangzhou 510640, China; University of Chinese Academy of Sciences, Beijing 100049, China*

**Chuhong Zhu** − *State Key Laboratory of Organic Geochemistry and Guangdong Key Laboratory of Environmental Protection and Resources Utilization, Guangzhou Institute of Geochemistry, Chinese Academy of Sciences, Guangzhou 510640, China; CAS Center for Excellence in Deep Earth Science, Guangzhou 510640, China; University of Chinese Academy of Sciences, Beijing 100049, China*

**Zihe Ren** − *State Key Laboratory of Organic Geochemistry and Guangdong Key Laboratory of Environmental Protection and Resources Utilization, Guangzhou Institute of Geochemistry, Chinese Academy of Sciences, Guangzhou 510640, China; CAS Center for Excellence in Deep Earth Science, Guangzhou 510640, China; University of Chinese Academy of Sciences, Beijing 100049, China*

**Yin-E Liu** − *State Key Laboratory of Organic Geochemistry and Guangdong Key Laboratory of Environmental Protection and Resources Utilization, Guangzhou Institute of Geochemistry, Chinese Academy of Sciences, Guangzhou 510640, China; CAS Center for Excellence in Deep Earth Science, Guangzhou 510640, China; University of Chinese Academy of Sciences, Beijing 100049, China*

**Shutao Gao** − *State Key Laboratory of Organic Geochemistry and Guangdong Key Laboratory of Environmental Protection and Resources Utilization and Guangdong-Hong Kong-*

*Macao Joint Laboratory for Environmental Pollution and Control, Guangzhou Institute of Geochemistry, Chinese Academy of Sciences, Guangzhou 510640, China; CAS Center for Excellence in Deep Earth Science, Guangzhou 510640, China*

**Yankuan Tian** − *State Key Laboratory of Organic Geochemistry and Guangdong Key Laboratory of Environmental Protection and Resources Utilization and Guangdong-Hong Kong-Macao Joint Laboratory for Environmental Pollution and Control, Guangzhou Institute of Geochemistry, Chinese Academy of Sciences, Guangzhou 510640, China; CAS Center for Excellence in Deep Earth Science, Guangzhou 510640, China*

**Xiaojun Luo** − *State Key Laboratory of Organic Geochemistry and Guangdong Key Laboratory of Environmental Protection and Resources Utilization and Guangdong-Hong Kong-Macao Joint Laboratory for Environmental Pollution and Control, Guangzhou Institute of Geochemistry, Chinese Academy of Sciences, Guangzhou 510640, China; CAS Center for Excellence in Deep Earth Science, Guangzhou 510640, China;* ⊙ orcid.org/0000-0002-2572-8108

**Bixian Mai** − *State Key Laboratory of Organic Geochemistry and Guangdong Key Laboratory of Environmental Protection and Resources Utilization and Guangdong-Hong Kong-Macao Joint Laboratory for Environmental Pollution and Control, Guangzhou Institute of Geochemistry, Chinese Academy of Sciences, Guangzhou 510640, China; CAS Center for Excellence in Deep Earth Science, Guangzhou 510640, China;* ⊙ orcid.org/0000-0001-6358-8698

Complete contact information is available at:
https://pubs.acs.org/10.1021/acs.est.1c00726

**Author Contributions**

C.H.: Experimenter, data analysis, writing; Y.Z.: Supervision, reviewing, editing; Y.C., C.Z., Y.-E.L., and Z.R.: Assistance; S.G. and Y.T.: Equipment debugging; X.L. and B.M.: Supervision, funding acquisition.

**Notes**

The authors declare no competing financial interest.

## ■ REFERENCES

(1) Chen, D.; Hale, R. C.; Letcher, R. J. Photochemical and Microbial Transformation of Emerging Flame Retardants: Cause for Concern? *Environ. Toxicol. Chem.* **2015**, *34*, 687−699.

(2) Breivik, K.; Sweetman, A.; Pacyna, J. M.; Jones, K. C. Towards a global historical emission inventory for selected PCB congeners - A mass balance approach-3 An update. *Sci. Total. Environ.* **2007**, *377*, 296−307.

(3) UNEP, 2017. The 16 new POPs. http://chm.pops.int/TheConvention/ThePOPs/AllPOPs/tabid/2509/Default.aspx (accessed January 31, 2021).

(4) Mao, S. D.; Zhang, G.; Zhao, S. Z.; Li, J.; Liu, X.; Cheng, Z. N.; Zhong, G. C.; Malik, R. N.; Liu, X. High Abundance of Unintentionally Produced Tetrachlorobiphenyls (PCB47/48/75, 51, and 68) in the Atmosphere at a Regional Background Site in East China. *Environ. Sci. Technol.* **2019**, *53*, 3464−3470.

(5) Zhao, S.; Jones, K. C.; Li, J.; Sweetman, A. J.; Liu, X.; Xu, Y.; Wang, Y.; Lin, T.; Mao, S.; Li, K.; Tang, J.; Zhang, G. Evidence for Major Contributions of Unintentionally Produced PCBs in the Air of China: Implications for the National Source Inventory. *Environ. Sci. Technol.* **2020**, *54*, 2163−2171.

(6) Zeng, Y. H.; Tang, B.; Luo, X. J.; Zheng, X. B.; Peng, P. A.; Mai, B. X. Organohalogen pollutants in surface particulates from workshop floors of four major e-waste recycling sites in China and implications for emission lists. *Sci. Total Environ.* **2016**, *569-570*, 982−989.

(7) Li, X.; Zhang, C.; Wang, K.; Lehmler, H. J. Fatty liver and impaired hepatic metabolism alter the congener-specific distribution of polychlorinated biphenyls (PCBs) in mice with a liver-specific deletion of cytochrome P450 reductase. *Environ. Pollut.* **2020**, *266*, No. 115233.

(8) Onozuka, D.; Nakamura, Y.; Tsuji, G.; Furue, M. Cancer- and noncancer-specific cumulative incidence of death after exposure to polychlorinated biphenyls and dioxins: A competing risk analysis among Yusho patients. *Environ. Int.* **2021**, *147*, 106320−106320.

(9) Li, C.; Liu, J.; Wu, N.; Pan, X.; Feng, J.; Al-Basher, G.; Allam, A. A.; Qu, R.; Wang, Z. Photochemical formation of hydroxylated polychlorinated biphenyls (OH-PCBs) from decachlorobiphenyl (PCB-209) on solids/air interface. *J. Hazard. Mater.* **2019**, *378*, No. 120758.

(10) Tang, T.; Zheng, Z.; Wang, R.; Huang, K.; Li, H.; Tao, X.; Dang, Z.; Yin, H.; Lu, G. Photodegradation behaviors of polychlorinated biphenyls in methanol by UV-irradiation: Solvent adducts and sigmatropic arrangement. *Chemosphere* **2018**, *193*, 861−868.

(11) Huang, C. C.; Zeng, Y. H.; Luo, X. J.; Ren, Z. H.; Tian, Y. K.; Mai, B. X. Comprehensive exploration of the ultraviolet degradation of polychlorinated biphenyls in different media. *Sci. Total Environ.* **2021**, *755*, 142590−142590.

(12) Huang, C. C.; Zeng, Y. H.; Luo, X. J.; Ren, Z. H.; Lu, Q. H.; Tian, Y. K.; Gao, S. T.; Wang, S. Q.; Harrad, S.; Mai, B. X. Tracing the sources and microbial degradation of PCBs in field sediments by a multiple-line-of-evidence approach including compound-specific stable isotope analysis. *Water Res.* **2020**, *182*, 115977−115977.

(13) Mai, B. X.; Zeng, E. Y.; Luo, X. J.; Yang, Q. S.; Zhang, G.; Li, X. D.; Sheng, G. Y.; Fu, J. M. Abundances, depositional fluxes, and homologue patterns of polychlorinated biphenyls in dated sediment cores from the Pearl River Delta. *China. Environ. Sci. Technol.* **2005**, *39*, 49−56.

(14) Zakon, Y.; Halicz, L.; Gelman, F. Bromine and Carbon Isotope Effects during Photolysis of Brominated Phenols. *Environ. Sci. Technol.* **2013**, *47*, 14147−14153.

(15) Liu, X.; Wu, L.; Kuemmel, S.; Merbach, I.; Lal, R.; Richnow, H. H. Compound-Specific Isotope Analysis and Enantiomer Fractionation to Characterize the Transformation of Hexachlorocyclohexane Isomers in a Soil-Wheat Pot System. *Environ. Sci. Technol.* **2020**, *54*, 8690−8698.

(16) Chevallier, M. L.; Cooper, M.; Kuemmel, S.; Barbance, A.; Le Paslier, D.; Richnow, H. H.; Saaidi, P. L.; Adrian, L. Distinct Carbon Isotope Fractionation Signatures during Biotic and Abiotic Reductive Transformation of Chlordecone. *Environ. Sci. Technol.* **2018**, *52*, 3615−3624.

(17) Zwank, L.; Berg, M.; Elsner, M.; Schmidt, T. C.; Schwarzenbach, R. P.; Haderlein, S. B. New evaluation scheme for two-dimensional isotope analysis to decipher biodegradation processes: Application to groundwater contamination by MTBE (vol 39, pg 1018, 2005). *Environ. Sci. Technol.* **2005**, *39*, 7344−7344.

(18) Penning, H.; Cramer, C. J.; Elsner, M. Rate-Dependent Carbon and Nitrogen Kinetic Isotope Fractionation in Hydrolysis of Isoproturon. *Environ. Sci. Technol.* **2008**, *42*, 7764−7771.

(19) Lihl, C.; Douglas, L. M.; Franke, S.; Perez-de-Mora, A.; Meyer, A. H.; Daubmeier, M.; Edwards, E. A.; Nijenhuis, I.; Lollar, B. S.; Elsner, M. Mechanistic Dichotomy in Bacterial Trichloroethene Dechlorination Revealed by Carbon and Chlorine Isotope Effects. *Environ. Sci. Technol.* **2019**, *53*, 4245−4254.

(20) Heckel, B.; Phillips, E.; Edwards, E.; Lollar, B. S.; Elsner, M.; Manefield, M. J.; Lee, M. Reductive Dehalogenation of Trichloromethane by Two Different Dehalobacter restrictus Strains Reveal Opposing Dual Element Isotope Effects. *Environ. Sci. Technol.* **2019**, *53*, 2332−2343.

(21) Liu, Y.; Liu, J.; Renpenning, J.; Nijenhuis, I.; Richnow, H. H. Dual C-Cl Isotope Analysis for Characterizing the Reductive Dechlorination of alpha- and gamma-Hexachlorocyclohexane by Two Dehalococcoides mccartyi Strains and an Enrichment Culture. *Environ. Sci. Technol.* **2020**, *54*, 7250−7260.

(22) Passeport, E.; Zhang, N.; Wu, L.; Herrmann, H.; Sherwood Lollar, B.; Richnow, H. H. Aqueous photodegradation of substituted chlorobenzenes: Kinetics, carbon isotope fractionation, and reaction mechanisms. *Water Res.* **2018**, *135*, 95−103.

(23) Ratti, M.; Canonica, S.; McNeill, K.; Erickson, P. R.; Bolotin, J.; Hofstetter, T. B. Isotope Fractionation Associated with the Direct Photolysis of 4-Chloroaniline. *Environ. Sci. Technol.* **2015**, *49*, 4263−4273.

(24) Hartenbach, A. E.; Hofstetter, T. B.; Tentscher, P. R.; Canonica, S.; Berg, M.; Schwarzenbach, R. P. Carbon, hydrogen, and nitrogen isotope fractionation during light-induced transformations of atrazine. *Environ. Sci. Technol.* **2008**, *42*, 7751−7756.

(25) Wang, X. W.; Hu, X. F.; Zhang, H.; Chang, F.; Luo, Y. M. Photolysis Kinetics, Mechanisms, and Pathways of Tetrabromobisphenol A in Water under Simulated Solar Light Irradiation. *Environ. Sci. Technol.* **2015**, *49*, 6683−6690.

(26) Ratti, M.; Canonica, S.; McNeill, K.; Bolotin, J.; Hofstetter, T. B. Isotope Fractionation Associated with the Indirect Photolysis of Substituted Anilines in Aqueous Solution. *Environ. Sci. Technol.* **2015**, *49*, 12766−12773.

(27) Ratti, M.; Canonica, S.; McNeill, K.; Bolotin, J.; Hofstetter, T. B. Isotope Fractionation Associated with the Photochemical Dechlorination of Chloroanilines. *Environ. Sci. Technol.* **2015**, *49*, 9797−9806.

(28) Ren, Z. H.; Zeng, Y. H.; Luo, X. J.; Huang, C. C.; Tian, Y. K.; Gao, S. T.; Mai, B. X. Observable carbon isotope fractionation in the photodegradation of polybrominated diphenyl ethers by simulated sunlight. *Chemosphere* **2021**, *266*, 128950−128950.

(29) Rosenfelder, N.; Bendig, P.; Vetter, W. Stable carbon isotope analysis (delta C-13 values) of polybrominated diphenyl ethers and their UV-transformation products. *Environ. Pollut.* **2011**, *159*, 2706−2712.

(30) Eriksson, J.; Green, N.; Marsh, G.; Bergman, Å. Photochemical decomposition of 15 polybrominated diphenyl ether congeners in methanol/water. *Environ. Sci. Technol.* **2004**, *38*, 3119−3125.

(31) Wang, J.; Chen, S. J.; Nie, X.; Tian, M.; Luo, X. J.; An, T. C.; Mai, B. X. Photolytic degradation of decabromodiphenyl ethane (DBDPE). *Chemosphere* **2012**, *89*, 844−849.

(32) Pan, Y. H.; Tsang, D. C. W.; Wang, Y. Y.; Li, Y.; Yang, X. The photodegradation of polybrominated diphenyl ethers (PBDEs) in various environmental matrices: Kinetics and mechanisms. *Chem. Eng. J.* **2016**, *297*, 74−96.

(33) Huang, C. C.; Tian, Y. K.; Zeng, Y. H.; Ren, Z. H.; Luo, X. J.; Mai, B. X. Chlorine and Bromine Isotope Analysis of Polychlorinated Biphenyls and Polybrominated Diphenyl Ethers Using Gas Chromatography-Quadrupole Mass Spectrometry. *J. Chromatogr. A* **2020**, *1634*, 461715−461715.

(34) Rayne, S.; Forest, K.; Friesen, K. J. Mechanistic aspects regarding the direct aqueous environmental photochemistry of phenol and its simple halogenated derivatives. A review. *Environ. Int.* **2009**, *35*, 425−437.

(35) Hunkeler, D.; Van Breukelen, B. M.; Elsner, M. Modeling Chlorine Isotope Trends during Sequential Transformation of Chlorinated Ethenes. *Environ. Sci. Technol.* **2009**, *43*, 6750−6756.

(36) Horii, Y.; Kannan, K.; Petrick, G.; Gamo, T.; Falandysz, J.; Yamashita, N. Congener-specific carbon isotopic analysis of technical PCB and PCN mixtures using two-dimensional gas chromatography-isotope ratio mass spectrometry (vol 54, pg 361, 2005). *Environ. Sci. Technol.* **2006**, *40*, 7952−7952.

(37) Elsner, M.; Imfeld, G. Compound-specific isotope analysis (CSIA) of micropollutants in the environment - current developments and future challenges. *Curr. Opin. Biotechnol.* **2016**, *41*, 60−72.

(38) Gauchotte-Lindsay, C.; Turnbull, S. M. On-line high-precision carbon position-specific stable isotope analysis: A review. *Trac-Trend. Anal. Chem.* **2016**, *76*, 115−125.

(39) Oliva, J. M.; Azenha, E. M. D. G.; Burrows, H. D.; Coimbra, R.; de Melo, J. S. S.; Canle, M. L.; Fernandez, M. I.; Santaballa, J. A.; Serrano-Andres, L. On the low-lying excited states of sym-triazine-based herbicides. *ChemPhysChem* **2005**, *6*, 306−314.

(40) Bernstein, A.; Shouakar-Stash, O.; Ebert, K.; Laskov, C.; Hunkeler, D.; Jeannottat, S.; Sakaguchi-Soeder, K.; Laaks, J.; Jochmann, M. A.; Cretnik, S.; Jager, J.; Haderlein, S. B.; Schmidt, T. C.; Aravena, R.; Elsner, M. Compound-Specific Chlorine Isotope Analysis: A Comparison of Gas Chromatography/Isotope Ratio Mass Spectrometry and Gas Chromatography/Quadrupole Mass Spectrometry Methods in an Interlaboratory Study. *Anal. Chem.* **2011**, *83*, 7624−7634.

(41) Torrento, C.; Palau, J.; Rodriguez-Fernandez, D.; Heckel, B.; Meyer, A.; Domenech, C.; Rosell, M.; Soler, A.; Elsner, M.; Hunkeler, D. Carbon and Chlorine Isotope Fractionation Patterns Associated with Different Engineered Chloroform Transformation Reactions. *Environ. Sci. Technol.* **2017**, *51*, 6174−6184.

(42) Elsner, M.; Zwank, L.; Hunkeler, D.; Schwarzenbach, R. P. A new concept linking observable stable isotope fractionation to transformation pathways of organic pollutants. *Environ. Sci. Technol.* **2005**, *39*, 6896−6916.

(43) Horst, A.; Renpenning, J.; Richnow, H. H.; Gehre, M. Compound Specific Stable Chlorine Isotopic Analysis of Volatile Aliphatic Compounds Using Gas Chromatography Hyphenated with Multiple Collector Inductively Coupled Plasma Mass Spectrometry. *Anal. Chem.* **2017**, *89*, 9131−9138.

(44) Eriksson, J.; Rahm, S.; Green, N.; Bergman, A.; Jakobsson, E. Photochemical transformations of tetrabromobisphenol A and related phenols in water. *Chemosphere* **2004**, *54*, 117−126.

(45) Elsner, M.; Chartrand, M.; Vanstone, N.; Couloume, G. L.; Lollar, B. S. Identifying abiotic chlorinated ethene degradation: Characteristic isotope patterns in reaction products with nanoscale zero-valent iron. *Environ. Sci. Technol.* **2008**, *42*, 5963−5970.